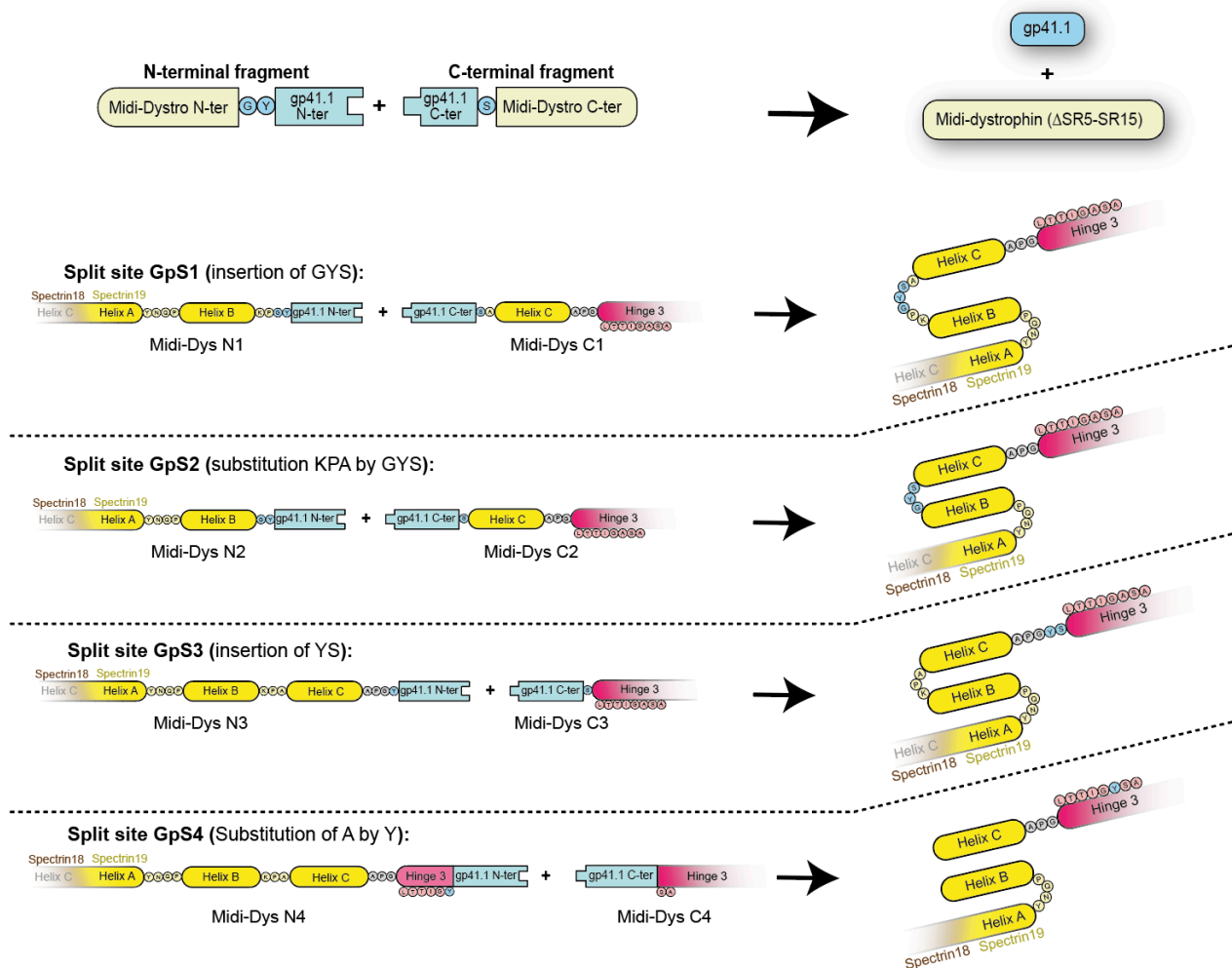
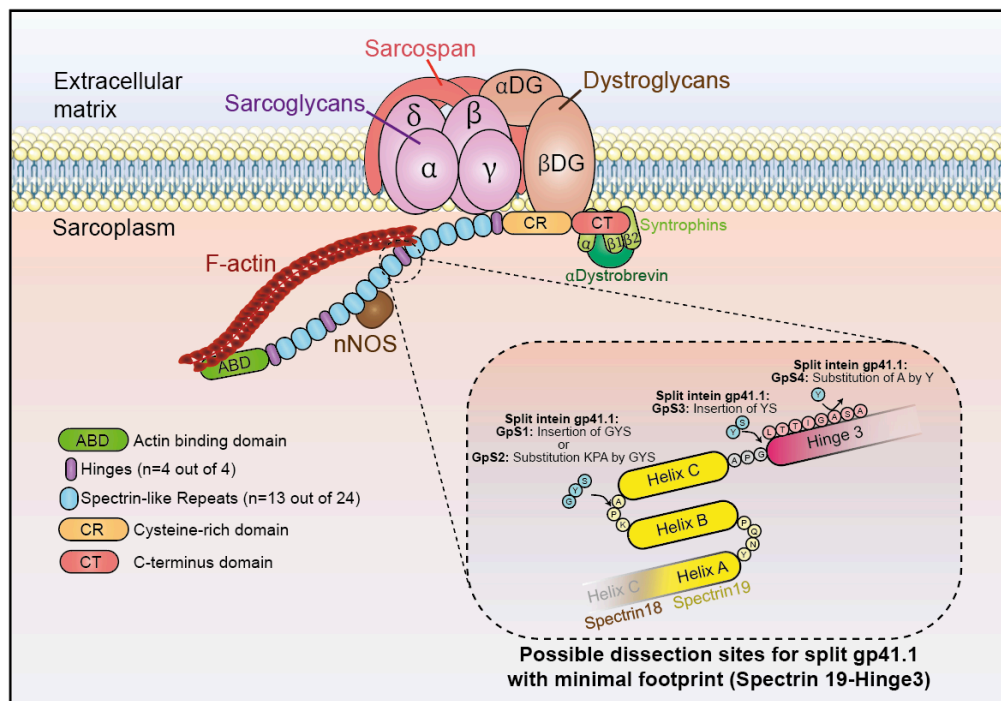


**Extended data Fig. 1: Validation of GFP as a platform for split intein screening.**

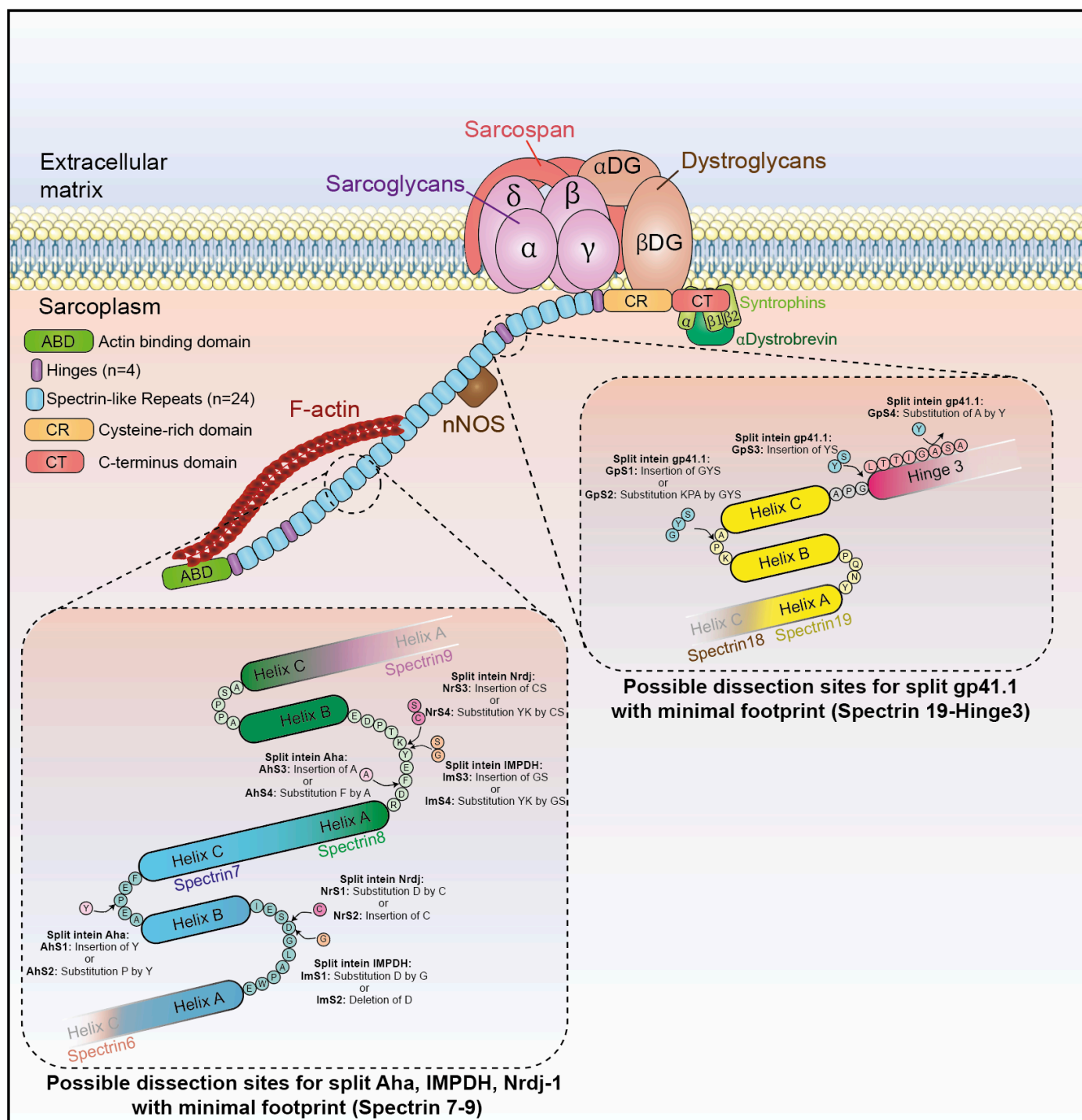
**a)** Diagram illustrating the topology of the GFP folding pattern with the chromophore, alpha helices, beta sheets, and the connecting loops with the two tested splitting sites (site#1: Glutamine 157-Lysine158, site#2: Glutamic acid 172-Aspartic acid 173). The numbers represent the delimiting residues at the beginning and the end of the secondary structures.

**b)** Mean fluorescence intensities of transfected HEK293 cells with either WT GFP or two mutated GFP harboring 8-amino acid insertions within the tested sites. **c)** Brightfield and fluorescent microscopy pictures of living HEK293 cells transfected with the WT or mutated GFP. Site#2 was more permissive to the insertion of an octapeptide and, thus, was selected as a splitting site where different split inteins were inserted for initial screening.



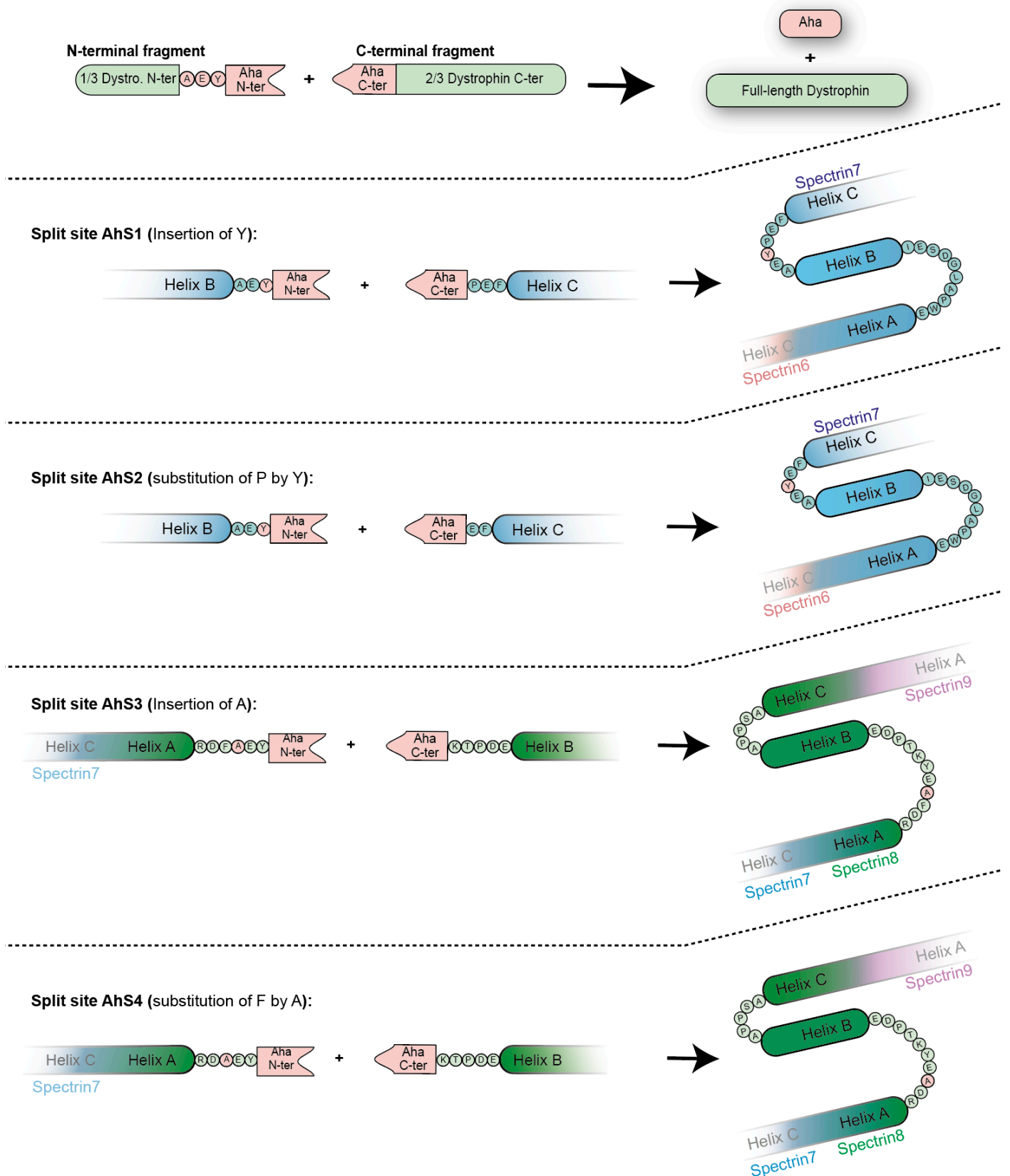
### Extended data Fig. 2: Illustration of splitting sites tested to generate the midi-Dys (ΔSR5-15) using split gp41.1.

Split gp41.1 with an optimized footprint (**Gly-Tyr/Ser**) was tested in four locations. The resulting midi-Dys (SR5-15) harbor a footprint of between one to three residues. These additional residues were inserted in loops between Helix B and C of Spectrin-like repeat 19, the linker between Helix C and Hinge 3, or within Hinge 3 to minimize their impact on protein folding.



**Extended data Fig. 3: Illustration splitting sites tested with triple AAV vector strategy to express the full-length dystrophin.**

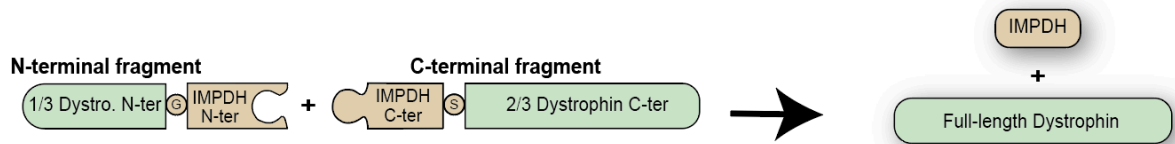
Optimized split Aha, IMPDH, and Nrdj1 with minimal footprints were inserted in loops located between Helix A & B or Helix B & C of Spectrin-like repeat 7 as well as Helix A & B of Spectrin-like repeat 8. These combinations join the N-terminal (from ABD to Spectrin-like repeat 7/8) to the middle fragment (from Spectrin-like repeat 7/8 to repeat 19/Hinge3). Split gp41.1 was evaluated to fuse the middle fragment to the C-terminal fragment at the same four splitting sites validated above with the dual strategy.



#### Extended data Fig. 4: Splitting sites tested with Aha.

Optimized split Aha with a minimal footprint (**Ala-Glu-Tyr**) was tested in four sites located in loops between Helix B & C of Spectrin-like repeat 7, or Helix A & B of Spectrin repeat 8. By using the native amino acids of dystrophin as part of the catalyzing reaction, the PTS mediated by the optimized Aha results in a minimal footprint with the insertion of only one residue (**Tyr** in AhS1 or AhS2, or **Ala** in AhS3 or AhS4).

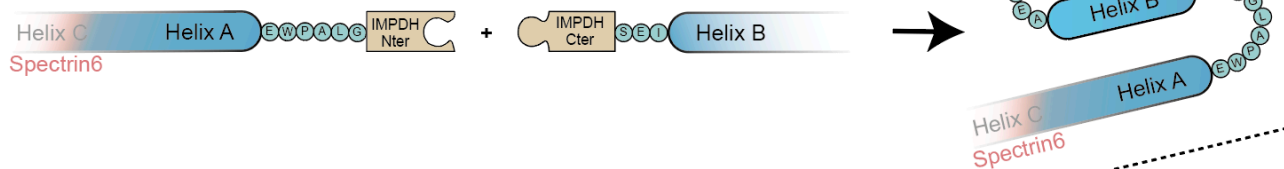




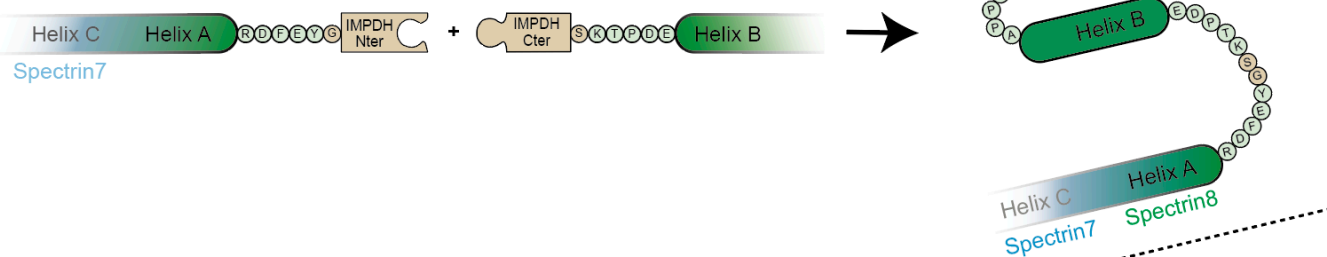
**Split site ImS1 (Substitution D by G):**



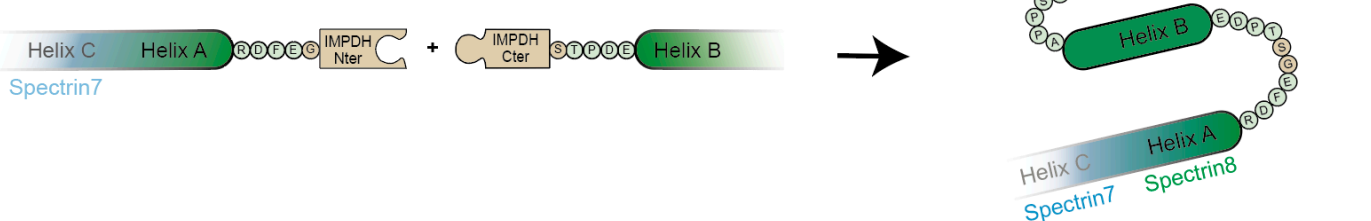
**Split site ImS2 (Deletion of D):**



**Split site ImS3 (Insertion of GS):**

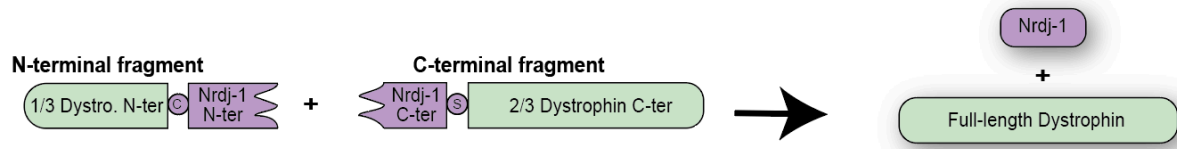


**Split site ImS4 (Substitution YK by GS):**

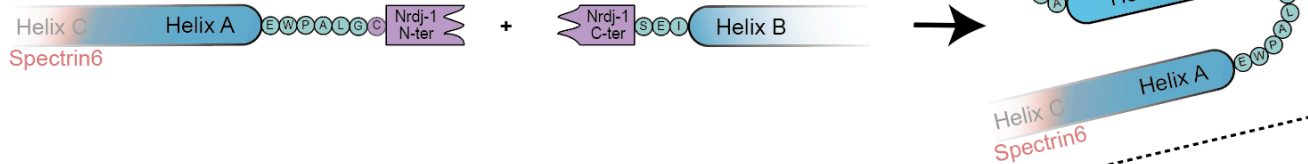


### Extended data Fig. 5: Splitting sites tested with IMPDH.

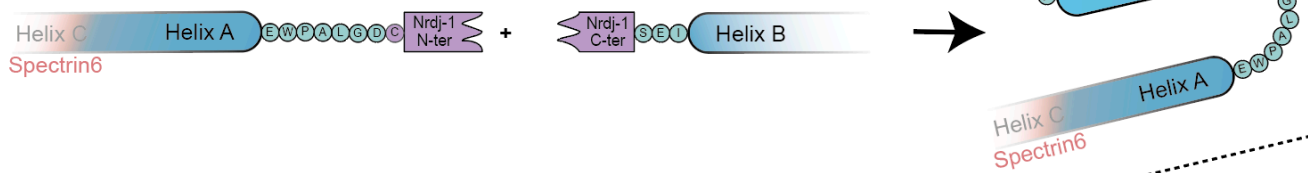
Optimized split IMPDH with a minimal footprint (**Gly/Ser**) was inserted in four sites located in loops between Helix A & B of Spectrin-like repeat 7 or Spectrin-like repeat 8. The PTS mediated by the optimized IMPDH results in a minimal footprint with the insertion of one (**Gly** in ImS1) or two residues (**Gly-Ser** in ImS3 & ImS4), while in ImS2 native **Gly** and **Ser** were used as catalyzing amino acids.



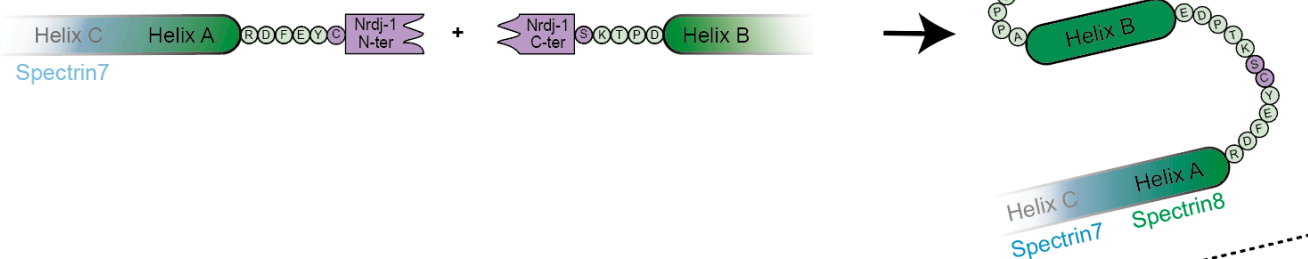
**Split site NrS1 (Substitution D by C):**



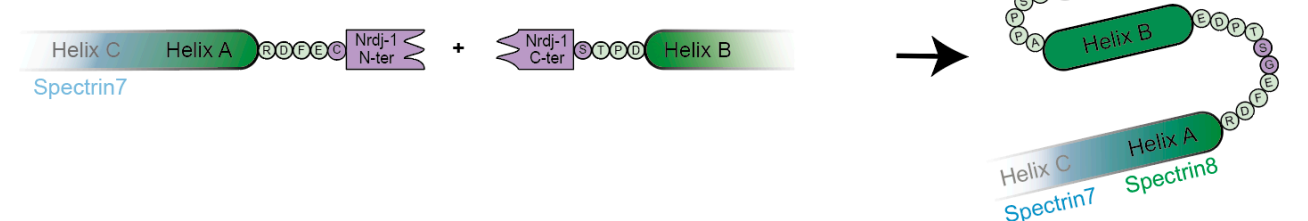
**Split site NrS2 (Insertion of C):**



**Split site NrS3 (Insertion of CS):**

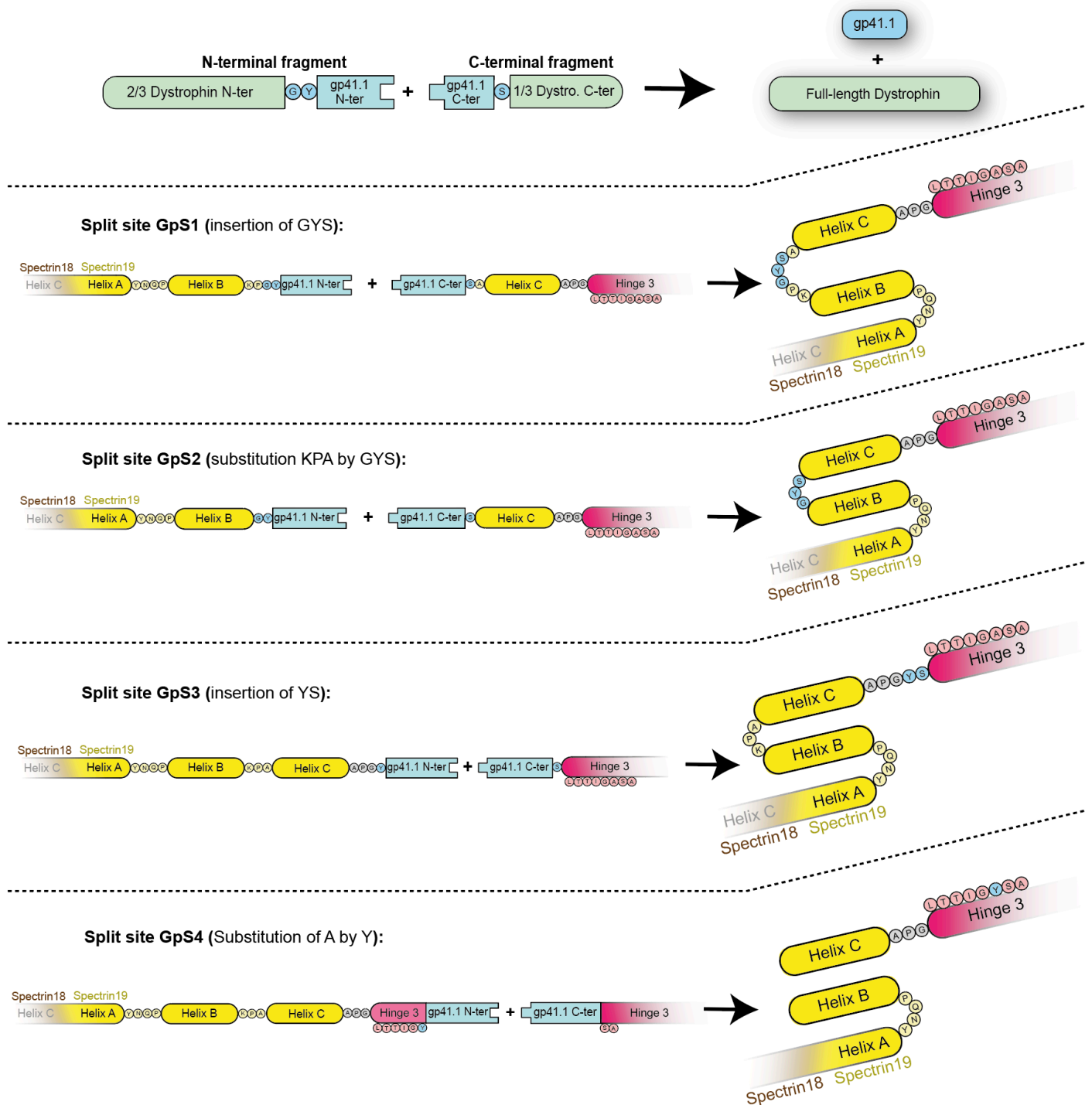


**Split site NrS4 (Substitution YK by CS):**



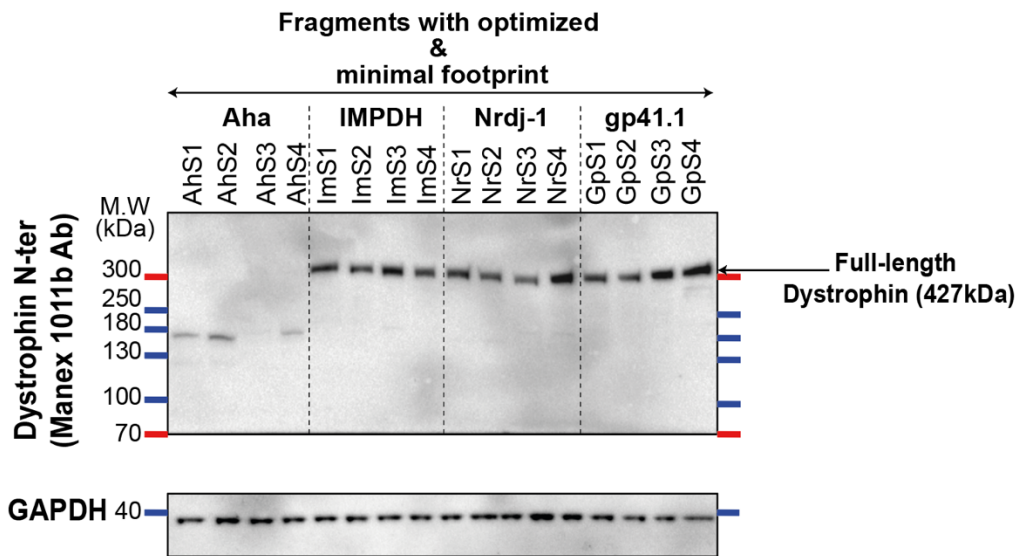
**Extended data Fig. 6: Splitting sites tested with Nrdj-1.**

The same splitting sites tested with IMPDH were evaluated with Nrdj-1. The PTS mediated by the optimized Nrdj-1 results in a minimal footprint with either substitution of the native Asp (D) by Cys (in NrS1), or insertion of a new residue (Cys in NrS2). Similarly, two residues (Cys-Ser) were inserted in NrS3 in the loop between Helix A and B of Spectrin repeat 8, while in NrS4 substitution of native Tyr-lys (K) by the footprint (Cys-Ser).



### Extended data Fig. 7: Splitting sites tested with gp41.1 in triple vector strategy.

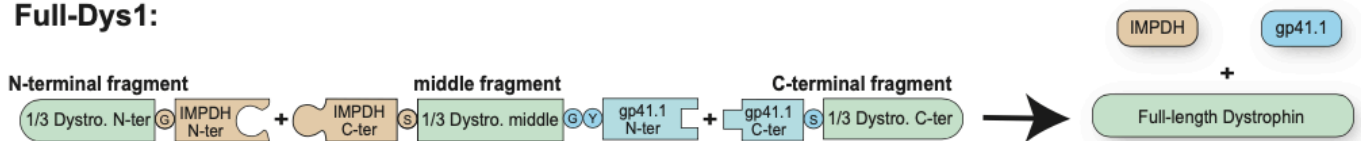
Optimized split gp41.1 was tested to join an N-terminal dystrophin fragment carrying two-thirds of the protein (from ABD to Spectrin-like repeat 19/Hinge 3) to the C-terminal one-third of dystrophin (from Spectrin-like repeat 19/Hinge 3 to C-terminus) using the same split sites used to reconstitute the midi-Dys (SR5-15).



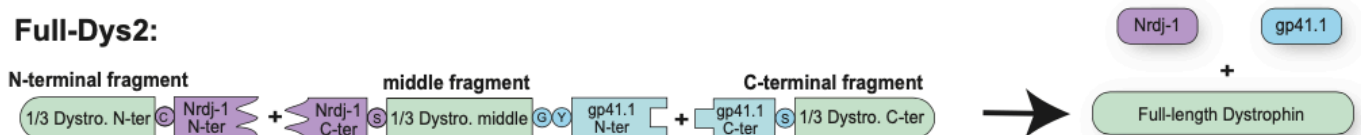
**Extended data Fig. 8: Evaluation of PTS to express full-length dystrophin using the optimized split inteins.**

The efficacy of each split intein to reconstitute full-length dystrophin from two fragments (one-third + two-thirds of dystrophin) was evaluated *in vitro* at four splitting sites (as depicted in Extended data Fig. 4 to 7)

**Full-Dys1:**



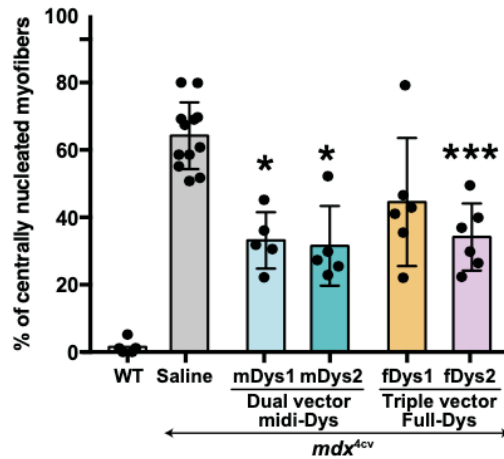
**Full-Dys2:**



**Extended data Fig. 9: Illustration of two combinations tested in the triple vector approach.**

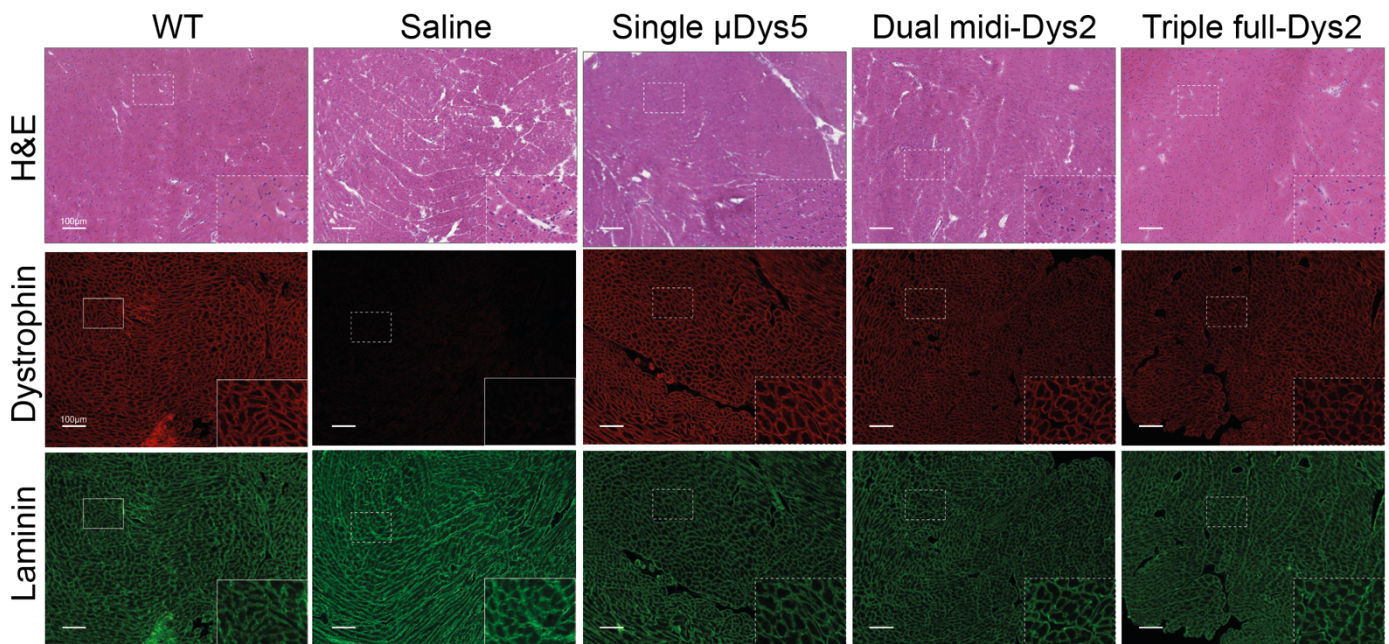
Two split inteins, IMPDH (split site: ImS4) and Nrdj-1 (split site: NrS4), were selected from previous screenings and tested for their ability to join the N-terminal to the middle fragment in a triple vector strategy. Split gp41.1 was inserted at the GpS4 split site to join the middle fragment to the C-terminal fragment.





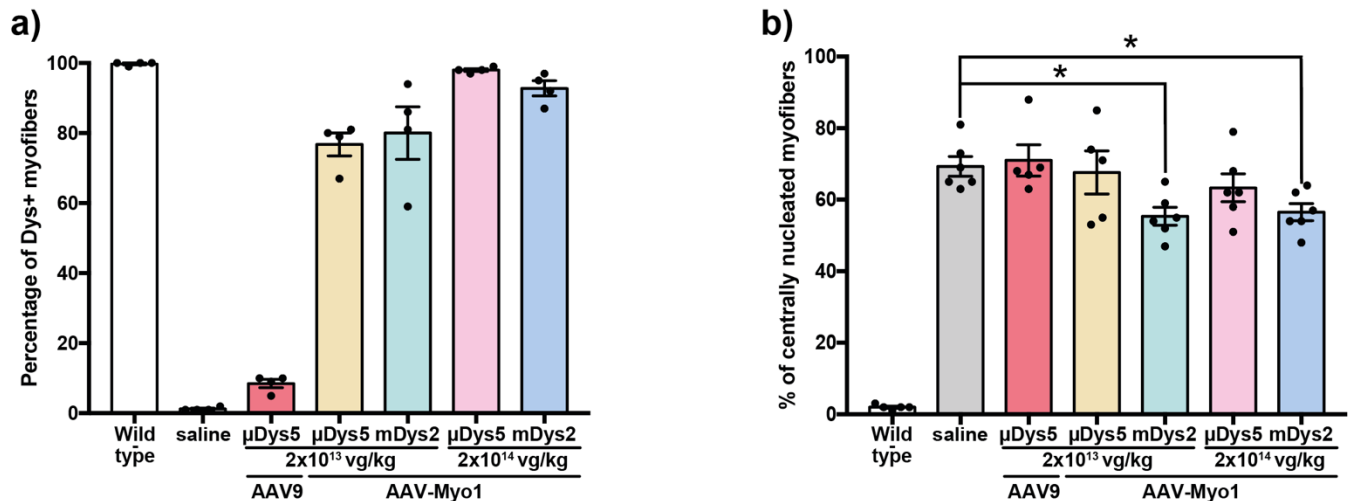
**Extended data Fig. 10: Quantification of myofibers with central nuclei following 5 weeks post AAV6 intramuscular injection:**

Using TA cross-section stained with H&E, the percentage of myofibers with centrally-located nuclei was determined ( $n=5-8$  sample per condition, ~400 myofibers were counted per sample). Data represent mean  $\pm$  s.e.m. \* $p<0.05$ , \*\*\* $p<0.001$  for mice treated AAV versus saline group (ANOVA test followed by Dunnett's post hoc).



**Extended data Fig. 11: General morphology and wide-spread expression of dystrophins in hearts.**

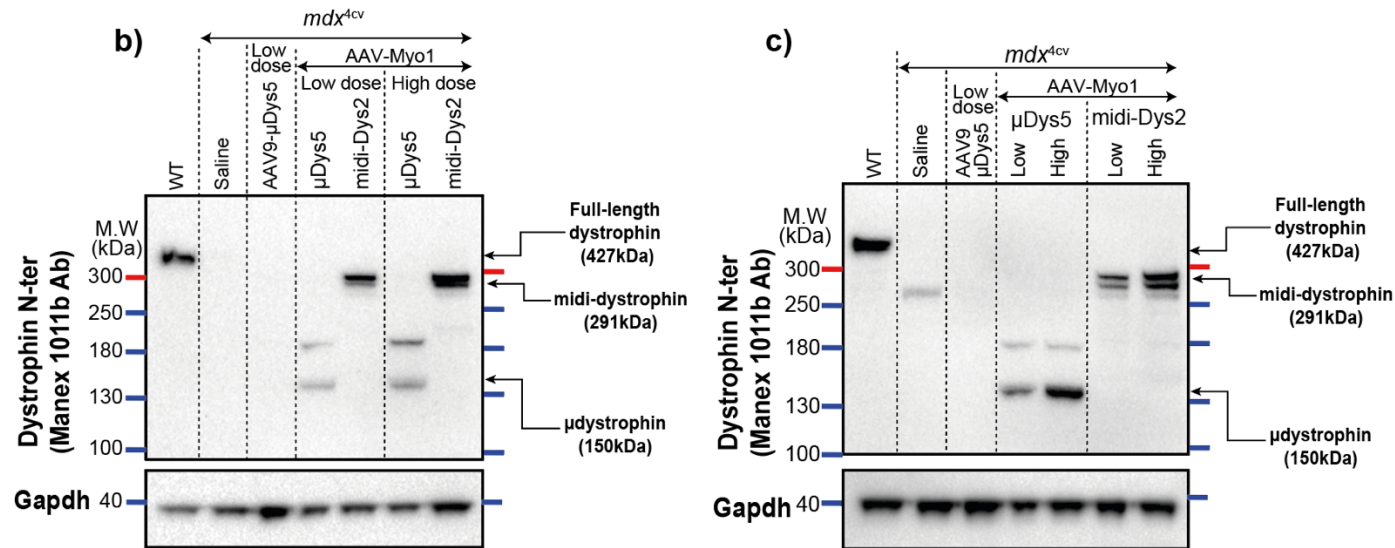
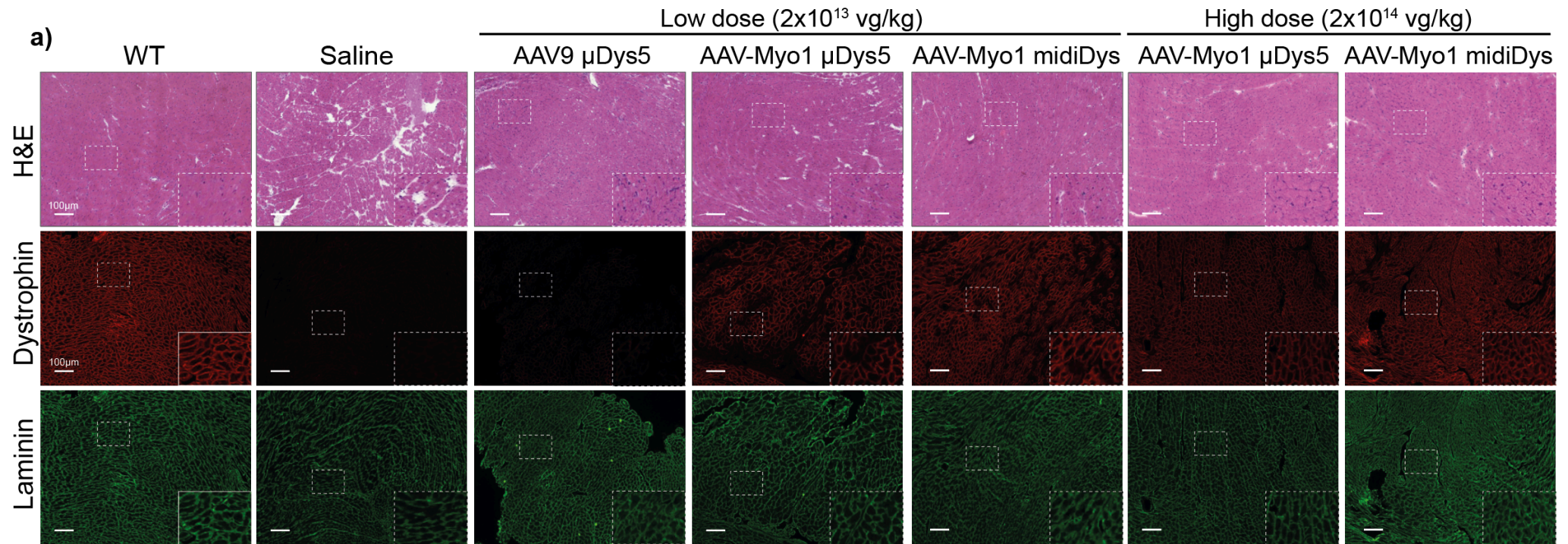
Heart sections of control mice or  $mdx^{4cv}$  males treated with single, dual, or triple AAV6 vectors stained with H&E or double-immunolabeled for dystrophin and laminin (Scale bars: 100 $\mu$ m).



**Extended data Fig. 12: Quantification of dystrophin biodistribution and centrally-nucleated myofibers across T.A muscle sections.**

**a)** Percentage of dystrophin-positive myofibers ( $n=4$ , more than 2000 fiber per each sample). **b)** Percentage of myofibers with central nuclei measured from cross-sections stained with H&E ( $n=5-6$ , ~300 fibers per sample). \* $p<0.05$  versus  $mdx^{4cv}$  mice treated with saline (ANOVA test followed by Dunnett's post hoc). μDys: micro-dystrophin. m-Dys: midi-dystrophin. Dys+: Dystrophin positive. vg: viral genome. kg: Kilogram





**Extended data Fig. 13:**

**a)** Heart transverse cryosections stained with H&E or immunolabelled for dystrophin and laminin (Scale bars: 100 $\mu$ m).

Western blot example of heart (**b**) and diaphragm (**c**) samples collected from mice treated with AAV9 or AAVMYO at a low or high dose and probed with antibodies against the N-terminal portion of dystrophin or Gapdh as a loading control.  $\mu$ Dys: micro-dystrophin. m-Dys: midi-dystrophin. Ab: antibody. kDa: kilodalton. MW: molecular weight.